NONSTEADY OSCILLATIONS OF A THIN ROD IN AN ELASTIC HALF SPACE

L. N. Yungerman

UDC 539.3

We solve the problem of the radiation of shearing waves by a thin cylindrical rod rigidly sealed into an elastic half space that is perpendicular to a free surface. In contrast to the steady formulation, on the basis of which the investigation of this kind of problem is usually carried out [1], we examine here the initial boundary-value problem which makes it possible to determine the extent to which nonsteadiness makes a contribution. Moreover, analysis of the nonsteady solutions is useful in regard to a number of questions related to engineering practice, including the problems of mining and construction, such as, for example, in evaluating soil and ground foundations for purposes of pile-driving operations, for evaluating the operation of powerful vibration generators that interact with the soil by means of anchor couplings.

1. Formulation of the Problem. An elastic rod of length ℓ and unit radius ($R_0 = 1$, $\ell \gg 1$) is sealed into an elastic half space $\{1 < r < \infty, z > 0\}$ so that its axis coincides with the z axis (Fig. 1). To the base of the rod $\{z = 0, r \leq 1\}$ at the zero instant of time the normal harmonic load $Q(t) = H_0(t)\sin\omega t$ [$H_0(t)$, i.e., the Heaviside function] is applied with the frequency $\omega \gg \ell/c$ (c is the velocity of the longitudinal wave in the rod). The embedded face $\{z = \ell, r \leq 1\}$ is free of stresses; the length of the wave traveling through the rod is given by $\lambda \gg 1$ ($\lambda \sim 2\pi c/\omega$). Under these assumptions, for purposes of describing the motion of the rod, a one-dimensional wave model with displacement V(t, z) is acceptable.

The problem of the oscillations of a rod sealed into an elastic half space reduces to the combined solution of a differential equation for the elastic rod, namely:

$$V_{tt} - V_{zz} + F(z, t) = 0 \tag{1.1}$$

and the equations for the dynamics of an elastic medium A

$$\begin{aligned} v_{tt} &= a^2 v_{zz} + b^2(v_{rr} + v_r/r) + (a^2 - b^2)(u_{rz} + u_z/r), \\ u_{tt} &= a^2(u_{rr} + u_r/r - u/r^2) + b^2 u_{zz} + (a^2 - b^2)v_{rz}. \end{aligned} \tag{1.2.1}$$

Here v(r, z, t) and u(r, z, t) are the axial and radial displacements of points in the medium; a and b are the velocities of the longitudinal and transverse waves; F(z, t) represents the reaction of the medium to the displacement of the rod. For the measurement units we have taken the radius R_0, the rod density ρ_0, and its Young's modulus E_0 (here the unit of velocity will be the speed of sound in the rod, while the unit of time will be the time within which the sound wave in the rod covers a distance equal to its radius).

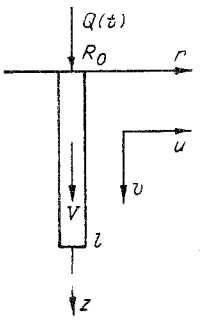

Fig. 1

Novosirbirsk. Translated from Zhurnal Prikladnoi Mekhaniki i Tekhnicheskoi Fiziki, No. 4, pp. 134-141, July-August, 1990. Original article submitted December 2, 1988; revision submitted March 24, 1989.

0021-8944/90/3104-0637$12.50

The solution of a number of dynamic problems with respect to the action of normal loads at the boundary of the half space [2, 3] shows that the strain amplitudes and their partial derivatives in the vertical direction significantly exceed the corresponding quantities in the radial direction. Assuming certain hypotheses with respect to the nature of these strains, this makes it possible to make the transition from the exact theory of elasticity for A to a physically adequate and mathematically simple model of a deformed medium with a single displacement B

$$v_{tt} = a^2 v_{zz} + b^2(v_{rr} + v_r/r), \tag{1.2.2}$$

which is used in the dynamic problems of unidirectional composites [4-6]. If we make an additional assumption to the effect that the shearing deformation of the soil is predominant, we come to the purely shear model of the medium C [7]

$$v_{tt} = b^2(v_{rr} + v_r/r). \tag{1.2.3}$$

We have also examined the plane variants of the above-enumerated models, and these are denoted A', B', and C'. In this case, we can derive an analytical solution for C', by means of which it is easy to analyze the influence of various parameters of the problem on the nature of the wave process. The qualitative proximity of the numerical solution for the plane and axisymmetric problems makes it possible to extend the derived results to the general case.

Let us assume that the surface of the half space is free of stresses, and that there exists a rigid contact between the rod and the medium. The reaction of the medium will then be determined by the shearing stress at the side surface of the rod

$$F(z, t) = -2\tau_{rz}|_{r=1}, \tag{1.3}$$

$\tau_{rz} = \rho b^2(v_r + u_z)$ in the model of A, $\tau_{rz} = \rho b^2 v_r$ in B and C; ρ is the relative density of the medium. The boundary conditions at the surface of the half space

$$\partial V/\partial z = Q(t) \ (z = 0, \ r \leqslant 1); \tag{1.4}$$

$$\sigma_z = \tau_{rz} = 0 \ (z = 0, \ r > 1). \tag{1.5}$$

In the B and C models Eq. (1.5) assumes the form of $\partial v/\partial z = 0$. The following condition of continuous displacement is imposed at the side surface of the rod:

$$V = v, \ u = 0 \ (r = 1). \tag{1.6}$$

The lower faces free of stresses

$$\partial V/\partial z = 0 \ (z = l). \tag{1.7}$$

To complete the formulation of the problem we have only to impose the conditions of radiation at infinity

$$u = v = 0 \ (\sqrt{r^2 + z^2} > at) \tag{1.8}$$

and to specify the initial conditions (without loss of generality, we will assume these to be zero)

$$u|_{t<0} = v|_{t<0} = V|_{t<0} = 0. \tag{1.9}$$

Thus, in the region $\{r > 0, z > 0\}$ we have to find the solution of Eqs. (1.1)-(1.2) with boundary conditions (1.3)-(1.8) and initial conditions (1.9).

2. The Analytical Solution. Initially we formulate the basic conclusions of the dispersion analysis for the approximate models. The set of eigenfrequencies (they are all complex) is identified as to model B, B', C, C' only in the region of the first several values. As the frequency number increases, its real part tends toward the corresponding eigenfrequency $\pi k/\ell$ for the oscillations of the free rod (for example, with $k = 4$ the difference is less than 1%). The imaginary part, characterizing the attenuation of the wave, tends to the quantity $-\gamma\sqrt{1 - a^2}$, where $\gamma = \rho b$. Thus, on excitation of the system at frequencies close to $\pi k/\ell$ resonances may arise. The appearance of the principal differences between the approximate models should be anticipated in the longwave region.

For the purely shearing plane model C' in the case of a stepped load given in the form of $Q(t) = H_0(t)$ an analytical solution has been found in [8], namely:

$$\dot{V}_H(t, z) = \sum_{n=0}^{\infty} \exp(-\gamma t)\{I_0(\gamma\sqrt{t^2-(z+2ln)^2})\,H_0(t-(z+2ln)) + \\ + I_0(\gamma\sqrt{t^2-(2l(n+1)-z)^2})\,H_0(t-(2l(n+1)-z))\}, \tag{2.1}$$

I_0 is the modified Bessel function. The solution for the case of sinusoidal load is found from (2.1) by means of the Duhamel integral

$$V(t, z) = \int_0^t \sin(\omega(t-\tau))\,\dot{V}_H(\tau, z)\,d\tau = \\ = \sum_{n=0}^{\infty}\left\{\int_{z_{1n}}^{t} \sin(\omega(t-\tau))\exp(-\gamma t)\,I_0\left(\gamma\sqrt{t^2-z_{1n}^2}\right)d\tau + \right. \\ \left. + \int_{z_{2n}}^{t} \sin(\omega(t-\tau))\exp(-\gamma t)\,I_0\left(\gamma\sqrt{t^2-z_{2n}^2}\right)d\tau\right\}, \\ z_{1n} = z + 2ln, \quad z_{2n} = 2l(n+1) - z. \tag{2.2}$$

For $t \gg z_*$ we can demonstrate the validity of the following asymptotic formula

$$\int_{z_*}^{t} \sin(\omega(t-\tau))\exp(-\gamma t)\,I_0\left(\gamma\sqrt{t^2-z_*^2}\right)d\tau \approx \\ \approx \exp(-\gamma t)\,I_0\left(\gamma\sqrt{t^2-z_*^2}\right)\frac{\omega}{\gamma^2+\omega^2} - \exp(-\gamma z_*)\cos\left(\omega(t-z_*) + \right. \\ \left. + \frac{\gamma}{\sqrt{\gamma^2+\omega^2}}\right)\frac{1}{\sqrt{\gamma^2+\omega^2}} \underset{\omega\gg\gamma}{\approx} \frac{1}{\omega}\left[\exp(-\gamma t)\,I_0\left(\gamma\sqrt{t^2-z_*^2}\right) - \right. \\ \left. - \exp(-\gamma z_*)\cos(\omega(t-z_*))\right]. \tag{2.3}$$

When we substitute (2.3) into (2.2) and if we limit ourselves to the first term of the sum, which is the same as taking the direct and first reflected waves into consideration, we find the asymptotic solution of the problem (1.1)-(1.9) with the model C', valid for large t, and as will be demonstrated later on, this solution is entirely acceptable for purposes of describing the results in practical cases:

$$V(t, z) = \frac{1}{\omega}\{[\exp(-\gamma t)\,I_0(\gamma\sqrt{t^2-z^2}) - \\ - \exp(-\gamma z)\cos(\omega(t-z))]\,H_0(t-z) + [\exp(-\gamma t)\,I_0(\gamma\sqrt{t^2-(2l-z)^2}) - \\ - \exp(-\gamma(2l-z))\cos(\omega(t+z-2l))]\,H_0(t+z-2l)\}. \tag{2.4}$$

The displacement in the direct wave, propagated through the rod, is defined by the first two terms in (2.4). The contribution due to nonsteadiness $\exp(-\gamma t)I_0(\gamma\sqrt{t^2-z^2})\times H_0(t-z)$ represents a function which instantaneously achieves its maximum value and then gradually diminishes exponentially over time (curve 2 in Fig. 2, $\lambda = 2\pi/\omega = 15$, $b = 0.1$, $a = 0$, $\rho = 0.3$, $\ell = 60$, $h_z = 1$). The second term is the perturbation at a carrier frequency with an amplitude constant in time and attenuating with increasing z. Only a single parameter of the medium is present in the solution, namely γ, which characterizes the attenuation of the function V(t, z). In the case of a semiinfinite rod solution (2.2) is substantially simplified and the asymptote is determined by the first two terms of formula (2.4).

3. Numerical Solution. For the numerical solution of Eqs. (1.1) and (1.2) we used the explicit "cross" type finite-difference scheme. The parasitic oscillations that arise on replacement of the differential equations by difference equations were eliminated by minimizing numerical dispersion [9].

Let us examine the system of finite-difference equations for the simplified models of the medium

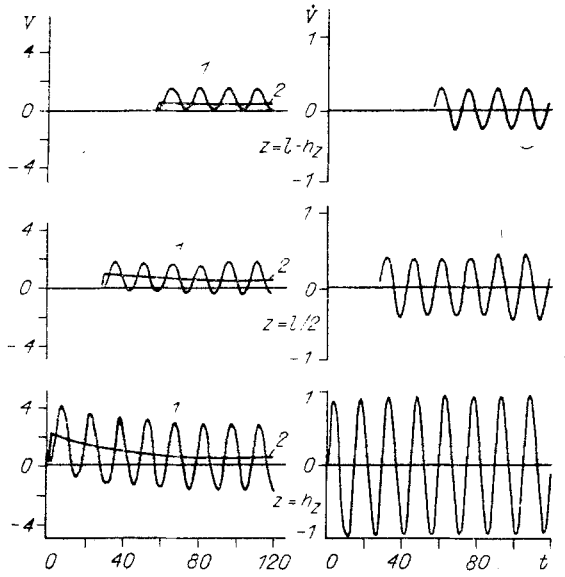

Fig. 2

$$m\frac{V_j^{n+1}-2V_j^n+V_j^{n-1}}{\tau^2}=\Lambda_{jj}V_j^n+G\frac{v_{j1}^n-V_j^n}{h_r}; \tag{3.1}$$

$$\frac{v_{ji}^{n+1}-2v_{ji}^n+v_{ji}^{n-1}}{\tau^2}=a^2\Lambda_{jj}v_{ji}^n+b^2\left(\Lambda_{ii}v_{ji}^n+d\frac{v_{ji}^n-v_{ji-1}^n}{2h_r(R+(i-1)h_r)}\right). \tag{3.2}$$

Here τ, h_r, and h_z are the intervals of the difference grid; Λ_{ii} and Λ_{jj} are the second-order difference operators with respect to the coordinates r(i) and z(j); m is the mass of the node; $G = 2\rho b^2$. When $a = 0$ we obtain the shearing models which when d = 1 or d = 0 are the axisymmetric and plane cases. The finite-difference equations for the exact theory of elasticity in A exhibits no fundamental differences from (3.2), but they are more cumbersome in notation and are therefore not presented here.

By means of standard Fourier analysis we derive the conditions of stability for scheme (3.1)

$$\tau\leqslant h_z\sqrt{m}(1+Gh_z^2/h_r^2)^{-1/2}, \tag{3.3}$$

for scheme (3.2)

$$\tau\leqslant\begin{cases}\left(\dfrac{a^2}{h_z^2}+\dfrac{b^2}{h_r^2}\right)^{-1/2} & (B,C),\\ \left[\max(a,b)\left(\dfrac{1}{h_z^2}+\dfrac{1}{h_r^2}\right)^{1/2}\right]^{-1} & (A).\end{cases}$$

The optimum parameters of the difference grid, providing for maximum approach of the regions relating the system of differential and finite-difference equations are, in the vertical direction,

$$h_z=\tau, \tag{3.4}$$

and in the radial direction

$$h_r=\begin{cases}\tau(b(1-(a\tau/h_z)^2)^{1/2})^{-1} & (B,C),\\ \tau(\max(a,b)(1-(a\tau/h_z)^2)^{1/2})^{-1} & (A).\end{cases}$$

It follows from (3.3) that (3.4) is satisfied only when $m = 1 + \varepsilon_m$ ($\varepsilon_m = Gh_z^2/h_r^2$), which corresponds to some mass connected to the rod. The existence of such a boundary layer corresponds to the physical essence of the problem; however, its magnitude in the given case is not connected to the physical characteristics of the process, but is dictated by the requirement of calculation stability. A rough estimate of the magnitude of the boundary

layer in the discrete model can be obtained from the conditions under which the rod moves together with the adjacent layer of the medium, having a thickness of $h_r/2$, so that $\tilde{m} = 1 + \tilde{\varepsilon}_m$ ($\tilde{\varepsilon}_m = \rho h_r/2$). In calculations of practical problems $\varepsilon_m < \tilde{\varepsilon}_m$.

In developing the numerical algorithm we find that the infinite region $\{z \geq 0\} \times \{r \geq 0\}$ is replaced by the finite region $\{0 \leq z \leq L\} \times \{0 \leq r \leq R\}$. The conditions of an absence of energy sources at infinity (1.8) can be replaced by the approximate conditions:

$$\frac{\partial v}{\partial r} = -\frac{1}{b}\frac{\partial v}{\partial t}\ (r = R), \quad \frac{\partial v}{\partial z} = -\frac{1}{a}\frac{\partial v}{\partial t}\ (z = L), \tag{3.5}$$

corresponding to the conditions of radiation in the one-dimensional case, where they follow directly out of the d'Alembert solution for a one-dimensional wave equation. In the A model the radial displacement condition should be added to this equation:

$$\frac{\partial u}{\partial r} = -\frac{1}{a}\frac{\partial u}{\partial t}\ (r = R), \quad \frac{\partial u}{\partial z} = -\frac{1}{b}\frac{\partial u}{\partial t}\ (z = L). \tag{3.6}$$

The question arises as to the extent to which (3.5) and (3.6) are exact. Let us note that for the shearing models C the first of the conditions in (3.5) becomes exact, while the second condition becomes extraneous, since there is no relationship between the horizontal layers of the medium ($\partial v/\partial z = 0$). Here, in the finite-difference algorithm there is no need to shift the boundary of the discrete region through any great distance (such that the wave reflected during the computation time does not reach the observation point). It is enough to take $L = \ell$, and in the radial direction to limit ourselves to several nodes of the grid. In B and B' conditions (3.5) become approximate and lead to the appearance of particular reflections from fictitious boundaries. However, as is shown by the calculations carried out over a broad range of parameters for the models B and B', the influence of these fictitious boundaries on the quantitative characteristics of the process is insignificant. However, the qualitative pattern of the oscillations does not change. Thus, with doubling ($L = 2\ell$) the numerical results change by no more than 1-2%. The distancing of the side boundary R from $5h_r$ to $30h_r$ yields an error of less than 5%. Considerably less exact are (3.5) and (3.6) in the A model. Here the regional boundary has to be shifted through a distance such that the wave reflected during the calculation time does not reach the observation point.

While the upper face of the rod is acted upon by the sinusoidal lobe $Q(t) = H_0(t) \times \sin(2\pi t/\lambda)$ the calculations are carried out until the process is stabilized with respect to time.

4. Comparison of the Models on the Basis of Calculation Results. The calculations have shown that the qualitative pattern of the oscillations is identical for all of the models. We will therefore limit ourselves to an examination of the C' model. Curves 1 in Fig. 2 represent oscillograms of the displacements at three points in the rod: near the surface of the half space ($z = h_z = 1$), in the middle of the rod ($z = \ell/2$), and near the lower face ($z = \ell - h_z$). To the right we see the velocity oscillograms. We can see that the closer the observation point to the bottom surface, the less energy the reflected wave carries to that surface, since in the propagation process a portion of the energy is scattered to the ambient medium. If the direct and reflected waves participate at point $z = \ell - h_z$ in the formation of amplitude, and if their contributions are approximately equal, then at the point $z = \ell/2$ on arrival of the reflected wave at the instant $t = 3\ell/2$ the amplitudes change only slightly (curve 2 describes the nonsteadiness contribution only for the direct wave). Let us note that the displacement calculated on the basis of the asymptote (2.4) coincides virtually with 1, the maximum difference in this computational example not exceeding 2%.

The results of the comparative analysis of the wave-process characteristics are shown in Table 1 ($V_m = \max_t |V(t, l)|$, $\dot{V}_m = \max_t |\dot{V}(t, l)|$, $b = 0.1$, $a = 0.2$, $\rho = 0.25$, $l = 60$, I representing the axisymmetric problem, while II represents the plane problem). Here we find the peak values of the displacements and velocities in the section $z = \ell$, where we observe the greatest quantitative differences between the models. The relative errors are shown alongside:

$$\varepsilon_{B,C} = \left|\frac{V_m^C - V_m^B}{V_m^C}\right| \cdot 100\ \%, \quad \varepsilon_{A',B',C'} = \max\left\{\left|\frac{V_m^{B'} - V_m^{A'}}{V_m^{A'}}\right|, \left|\frac{V_m^{C'} - V_m^{A'}}{V_m^{A'}}\right|\right\} \cdot 100\ \%,$$

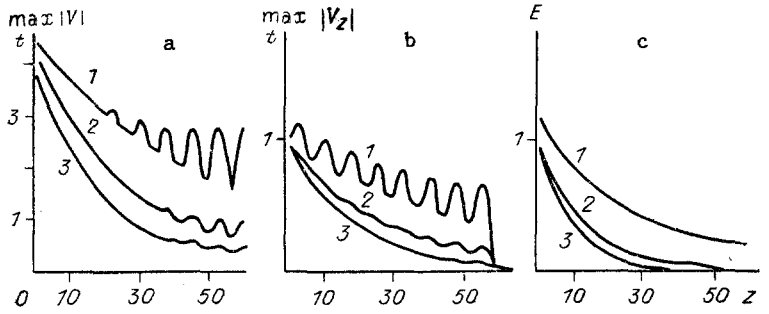

Fig. 3

TABLE 1

	I					II					
	λ	B	$\varepsilon_{B,C}$, %	C	$\varepsilon_{I,II}$, %	A'	$\varepsilon_{A',B',C'}$, %	B'	$\varepsilon_{B',C'}$, %	C'	(2.4)
V_m	$l/2$	2,97	1,6	2,92	28,8	4,06	1,2	4,10	1,2	4,09	4,05
	$l/3$	2,29	2,6	2,23	20,9	2,82	4,6	2,76	2,5	2,72	2,69
	$l/6$	1,17	9,3	1,29	8,6	1,56	2,5	1,28	3,1	1,24	1,26
$\dot{V}_m$	$l/2$	0,39	4,2	0,37	18	0,44	2,7	0,45	4,4	0,43	0,43
	$l/3$	0,48	5,2	0,45	10,4	0,46	10,4	0,45	7,3	0,42	0,42
	$l/6$	0,38	7,3	0,35	8,9	0,45	22,7	0,35	1,7	0,35	0,35

$\varepsilon_{I,II}$ represents the comparison among all proposed models, including that of asymptotic formula (2.4). These data correspond to calculations for three values of the wavelength $\lambda = l/2, l/3, l/6$. As was demonstrated in the dispersion analysis, the main differences between the plane and axisymmetric models are observed in the longwave region. On the other hand, the longer the wave, the closer the simplified models B and C to the exact elasticity theory for A. The differences among the models with a single displacement (B) and the purely shearing models (C) are insignificant over the entire range of oscillations. The difference in (2.4) from the numerical solution for the model C' does not exceed 3%.

Thus, the transition from A to B and C is entirely justified. In studying the qualitative behavior of the wave in the rod, we can use any of the models being discussed here. Having interpreted the numerical result in the longwave region, we have to distinguish between the plane and axisymmetric formulations. In the following, when studying the effect of geometric and physical parameters of the system on the wave process, we will take the B model as our basis.

5. Analysis of the Results. We can divide all of the wave-process parameters into three groups: a, b, and ρ are the relative physical parameters of the medium being investigated; l is the geometric parameter; and λ is the wavelength of the forces oscillations.

Let us initially examine the effect of the medium's parameters. As we can see from a comparative analysis of the models, the velocity of the expansion wave exerts virtually no influence on the wave pattern. Thus, with a change in a from 0 to 2b the maximum difference in oscillation amplitudes for the velocity amounts to 7% over the entire range of oscillations. It is natural that with an increase in a to magnitudes on the order of 6-10b the influence of this parameter becomes noticeable, but in the majority of actual media (for example, in soils, in rocks) no such velocity relationship is realized. Thus, the process of wave propagation through the rod depends only weakly on the velocity of the longitudinal wave in the ambient medium. If we are to speak of a solution of the inverse problem (i.e., finding the parameters of the medium from an analysis of the wave pattern in the rod), then the definition of a is problematical.

In the derived analytical solution of (2.2) and its asymptote (2.4) there exist two parameters, namely: ω is the frequency of the excited load and $\gamma = \rho b$ (ρ is the relative density of the medium, b is the relative velocity at which the shearing wave is propagated). It is natural to assume that with a fixed frequency it is precisely γ that will exert the most noticeable influence on the wave process. The numerical calculations conducted over

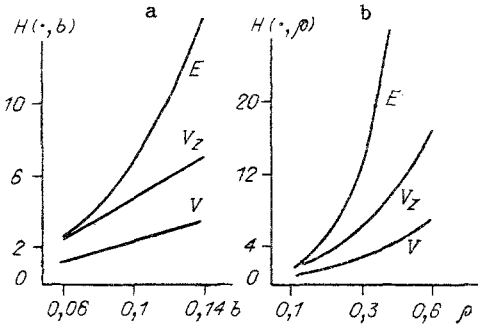

Fig. 4

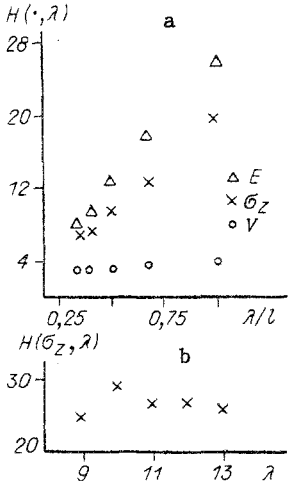

Fig. 5

TABLE 2

Model	λ					
	l/6	ε, %	l/3	ε, %	l/2	ε,%
B	0.02616	4,64	0,02797	11,9	0,03060	22,4
C	0,02670	6,8	0,02855	14,2	0,03106	24,2
A′	0,02143	14,3	0,02452	1,92	0,02520	0,8
B′	0,02457	1,72	0,0262	1,52	0,02468	1,28
C′	0,02507	0,28	0,02499	0,04	0,02487	0,52

a broad range of parameters completely confirmed this assumption. Figure 3 shows diagrams of the peak absolutely values of the displacements, stresses, and of the energy in sections of the rod as functions of the coordinate z. These curves correspond to various values of the medium's density ρ (1: 0.2; 2: 0.4; 3: 0.6). Figure 3 and all the subsequent figures (unless otherwise stipulated) all of the parameters are fixed: $\ell = 60$, $\lambda = \ell/4$, $\rho = 0.25$, $b = 0.1$, $a = 0.2$. We see that with an increase in density the attenuation of the wave characteristics increases. The wavelike nature of these curves is associated with the phase difference between the combining direct and reflected waves.

Let us introduce the functional $H(f, \beta)$, characterizing the attenuation of some wave function $f(z)$ on passage of the wave through the rod from the upper face to the lower face, for a given value of some parameter β:

$$H(f, \beta) = \max_t |f(0)| / \max_t |f(l)|.$$

For displacement and stress type functions diminishing nonmonotonically, we take the averaged quantity. Figure 4 shows the graphs of the attenuation of displacement and stress, as well as of energy, as functions of the various parameters of the problem. With increasing γ (corresponidngly, with increasing ρ and b) the function H increases monotonically for all basic amplitudes and energy characteristics of the wave process in the rod.

Figure 5a illustrates the function $H(\cdot, \lambda)$. The wavelength varies from $\ell/6$ to 2ℓ. As was to be expected, $H(\cdot, \lambda)$ increases with a rise in λ. The longer waves provide for better radiation into the medium, and all of the wave characteristics are rapidly attenuated. Nevertheless, owing to the presence of partial resonance the function $H(\cdot, \lambda)$ for certain wavelengths is not one increasing monotonically. Figure 5b, where the values of $H(\cdot, \lambda)$ are shown for $\lambda = 9, 10, 11, 12$, we see that at the resonance wavelength ($2\ell/\lambda \in \mathbf{Z}$) the attenuation is weaker.

The monotonic nature of attenuation in the amplitudes of the basic characteristics for the wave process allows us to make the transition to an examination of the inverse problem of determining the parameters of the ambient medium on the basis of the known wave pattern in the rod. The density ρ of the medium or the velocity b of the shearing wave may be the unknowns.

Thus, let the value of the functional H(f, β) be given for some characteristic of the wave process f(z). We have to find the unknown parameter β of the medium. For the solution of the inverse problem we have utilized (2.4):

$$H(V, \gamma) = \max_t |V^{ac}(0)| / \max_t |V^{ac}(l)| = h_0, \tag{5.1}$$

h_0 is obtained from numerical solution of the direct problem for various simplified models; λ is fixed in a manner such as to satisfy all limitations imposed in the introduction of the one-dimensional model of the rod and of the simplified models of the medium. The parameter γ is defined from (5.1). In the numerical experiment that we have carried out $\tilde{\gamma} = 0.025$. Table 2 shows the values of γ found from (5.1) in the solution of the inverse problem for various λ and the relative error in comparison to the true values of $\tilde{\gamma}$ ($\ell = 60$, $a = 2b$).

In conclusion let us formulate the main results. 1. The transition from the theory of elasticity to the simplified models of the medium has been validated in the description of nonsteady oscillations of an elastic rod in a half space. 2. We have analyzed the effect of the properties of the medium on the nature of the wave pattern in the rod and we have demonstrated that the fundamental parameters responsible for the attenuation of the oscillations are the frequency of the excited load, the density, and the shearing rigidity of the medium. The influence of volumetric rigidity is inconsequential. 3. In practical calculations, in the construction of solutions, it is possible to use approximate analytical estimates, such as those derived for the shearing model of the medium.

The author expresses his gratitude to Kh. B. Tkach for his formulation of the problem and to M. V. Stepanenko for his attention to this study and for his useful discussion.

LITERATURE CITED

1. V. T. Grinchenko and V. V. Meleshko, Harmonic Oscillations and Waves in Elastic Bodies [in Russian], Naukova Dumka, Kiev (1981).
2. Kh. A. Rakhmatulin, "The propagation of elastic-plastic waves in half space," Prikl. Mat. Mekh., 23, No. 3 (1959).
3. T. Ormonbekov, The Interaction of Structures with a Medium [in Russian], Ilim, Frunze (1983).
4. A. M. Mikhailov, "The dynamics of a unidirectional plastic," Zh. Prikl. Mekh. Tekh. Fiz., No. 4 (1974).
5. M. V. Stepanenko, "The dynamics of the destruction of a unidirectional plastic," Zh. Prikl. Mekh. Tekh. Fiz., No. 4 (1979).
6. M. V. Stepanenko, "A numerical experiment in the dynamics of composite-material destruction," Mekh. Kompozit. Mater., No. 1 (1981).
7. I. O. Outwater, Jr., "The mechanics of plastics reinforcement in tension," Modern Plastics, 33, No. 7 (1956).
8. A. M. Mikhailov, "Nonaxisymmetric dynamic loading of a shell with rigid reinforcing ribs," Izv. Akad. Nauk SSSR, Mekh. Tverd. Tela, No. 1 (1979).
9. S. A. Abdukadyrov, N. I. Pinchukova, and M. V. Stepanenko, "A numerical method for the solution of the equations of dynamics in elastic media and structures," FTPRPI, No. 6 (1984).